J|A|C|S

JOURNAL OF THE AMERICAN CHEMICAL SOCIETY

Article

Photodynamic Control of the Chain Length in Supramolecular Polymers: Switching an Intercalator into a Chain Capper

Elisabeth Weyandt, Gijs M. ter Huurne, Ghislaine Vantomme, Albert J. Markvoort, Anja R. A. Palmans, and E. W. Meijer*

Cite This: *J. Am. Chem. Soc.* 2020, 142, 6295−6303
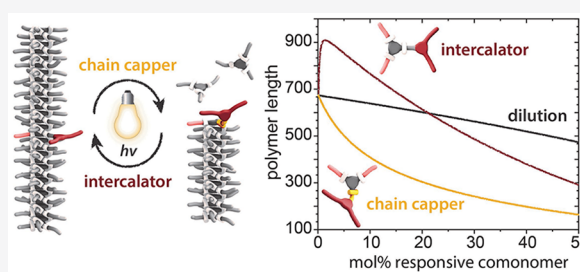
Read Online

ACCESS | Metrics & More | Article Recommendations | Supporting Information

ABSTRACT: Supramolecular systems are intrinsically dynamic and sensitive to changes in molecular structure and external conditions. Because of these unique properties, strategies to control polymer length, composition, comonomer sequence, and morphology have to be developed for sufficient control over supramolecular copolymerizations. We designed photoresponsive, mono acyl hydrazone functionalized benzene-1,3,5-tricarboxamide (**m-BTA**) monomers that play a dual role in the coassembly with achiral alkyl BTAs (**a-BTA**). In the *E* isomer form, the chiral **m-BTA** monomers intercalate into stacks of **a-BTA** and dictate the chirality of the helices. Photoisomerization to the *Z* isomer transforms the intercalator into a chain capper, allowing dynamic shortening of chain length in the supramolecular aggregates. We combine optical spectroscopy and light-scattering experiments with theoretical modeling to show the reversible decrease in length when switching from the *E* to *Z* isomer of **m-BTA** in the copolymer with inert **a-BTA**. With a mass-balance thermodynamic model, we gain additional insights into the composition of copolymers and length distributions of the species over a broad range of concentrations and mixing ratios of **a-BTA**/**m-BTA**. Moreover, the model was used to predict the impact of an additive (chain capper and intercalator) on the chain length over a range of concentrations, showing a remarkable amplification of efficiency at high concentrations. By employing a stimuli-responsive comonomer in a mostly inert polymer, we can cooperatively amplify the effect of the switching and obtain photocontrol of polymer length. Moreover, this dynamic decrease in chain length causes a macroscopic gel-to-sol phase transformation of the copolymer gel, although 99.4% of the organogel is inert to the light stimulus.

INTRODUCTION

Although the field of supramolecular polymers has made exciting progress, many challenges remain in controlling supramolecular copolymerization, morphologies, composition, and aggregate length.[1−3] When examining copolymerizations of two monomers, the influence of a second component on the length of the structures formed is often not considered. However, these features are of paramount importance for the resulting properties of the system and hence for their use in novel applications. A second component in supramolecular polymerizations can influence the degree of polymerization in many ways by acting as a comonomer, an intercalator, a sequestrator, or a chain capper. Controlling the chain length of isodesmic supramolecular polymers has been achieved by adding monotopic comonomers (chain cappers), which leads to an efficient reduction in chain length.[4−8] For cooperative supramolecular polymerization, however, the two reactive sites of the faces of the monomers are electronically coupled, leading to either monomeric and small species or long polymer chains coexisting in solution.[9] In recent years many elegant examples have been reported that achieved kinetic control over aggregate length by using pre-equilibrated seeds, tailored initiators, or metastable monomers.[10−14] In addition, previous studies have elegantly demonstrated the ability to control the polymerization and depolymerization of supramolecular homopolymers with light or other stimuli through the creation of defects and depolymerizing through the buildup of steric strain.[16,17]

In the field of molecular switches, stimuli-responsive molecules have been excessively studied to translate molecular conformational changes into macroscopic events in supramolecular polymers and liquid crystals (phase transitions or changes in aggregation affinity).[18−20] Although pH,[21] temperature, and magnetic as well as electric fields[22] are often exploited, light is by far the most popular stimulus as it offers excellent spatiotemporal resolution, it is green, and it can easily be dosed and controlled.[23−28] The types of systems that exhibit photoresponsive behavior can be broadly separated into three categories: (1) switching of single molecules in solution, (2)

Scheme 1. Molecular Structure of (a) Mono Acyl Hydrazone Functionalized BTA (m-BTA), (b) Achiral Octyl BTA (a-BTA) Monomers, and (c) Copolymer Formed by Intercalation of Chiral m-BTA into Helical Stacks of a-BTA
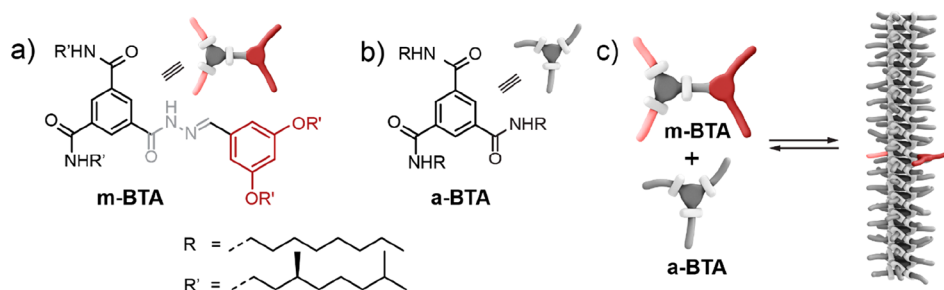
switching in supramolecular systems (e.g., fibers, tubes, gels, and micelles), and (3) switching in mobile bulk phases such as liquid crystals. For the switching in liquid crystal systems many examples have been reported where only dopant quantities (typically <5%) in an inert matrix are sufficient to induce responsive behavior of the overall materials.[29−33] For the switching in solution and in supramolecular system, however, usually all of the molecules composing the system contain the responsive unit undergoing photoisomerization.[16,34] To our knowledge, only few studies reported macroscopic effects from the isomerization of low molar quantities (5−10 mol %) of responsive monomers in a supramolecular coassembly.[35−40]

Benzene-1,3,5-tricarboxamide (BTA)-based supramolecular polymers are a unique class of monomers as they readily assemble and reach the thermodynamic equilibrium within a few seconds. Because of the simplicity of design and fast equilibration of the BTAs, they are an ideal system to study and understand the interactions with more complex molecules. Many groups are using this basic structure to unravel novel concepts in dynamic systems, while our group recently reported on the interaction of BTA monomers with supramolecular competitors as an alternative approach to regulate the length of supramolecular polymers.[15]

Here, we report on a supramolecular system sensitive to light although only minor quantities of its constituents are photoactive. The system is based on a two-component polymerization of chiral, mono acyl hydrazone functionalized BTAs (**m-BTA**) with achiral alkyl BTAs (**a-BTA**, Scheme 1). Acyl hydrazones are well-known for their use as conformational switches by metal coordination[41,42] and in dynamic combinatorial chemistry,[43−45] and they have also gained attention and popularity as a new class of modular and potent photoswitches.[30,46−50] They feature a complementary hydrogen bond donor/acceptor C(=O)−NH unit and a photoisomerizable C=N double bond.[51,52] Compared to other photochromic groups, they offer excellent stabilities as well as good efficiency and band separation and are readily accessible from commercially available starting materials.[47,53,54] We show how the acyl hydrazone monomers, although not able to form homopolymers, copolymerize with **a-BTA** into light-responsive copolymers. Photoisomerization of the **m-BTA** monomer from the *E* to the *Z* isomer transforms **m-BTA** from an intercalating comonomer to a supramolecular chain capper, effectively decreasing the degree of polymerization of the copolymers after light irradiation. The cooperativity of the **aBTA/m-BTA** copolymers allows the local changes in the chromophore structure to be amplified, thereby reversibly decreasing the degree of polymerization upon light irradiation.

RESULTS

Molecular Design, Synthesis, and Solid State Aggregation of BTA Monomers. We synthesized and characterized an acyl hydrazone BTA derivative (**m-BTA**) comprising one amide fused with an acyl hydrazone motif and studied its properties as a photoresponsive, supramolecular monomer (Scheme 1a). The two central core amides of **m-BTA** and the 3,5-position on the phenyl ring of the acyl hydrazone were functionalized with chiral (*S*)-3,7-dimethyloctyl alkyl chains to enhance solubility and introduce helical bias in the supramolecular polymer. The molecular structure of **m-BTA** features a similar self-complementary amide array as the achiral alkyl BTA (**a-BTA**, Scheme 1b),[55] therefore allowing us to study the homo- and copolymerization of both monomers. We hypothesize that the chiral **m-BTA** monomers will act as supramolecular sergeants,[56,57] dictating the helicity of the **a-BTA** soldier stacks, even at low molar percentages of additive (Scheme 1c).

The synthesis of **m-BTA** is described in the Supporting Information (Figures S1 and S2) and was conducted in good overall yield (71%). Commercially available 3,5-dihydroxybenzaldehyde was functionalized with (*S*)-3,7-dimethyloctyl side chains in a Williamson ether coupling. To get the final compounds, the mono methylbenzene carboxylate derivative was transformed into a hydrazide and reacted with the substituted aldehyde in an acid-catalyzed condensation reaction.[46,58] The synthesis of **a-BTA** has been reported previously.[55] The compounds were characterized by ^{1}H and ^{13}C NMR, MALDI-TOF, and FT-IR.

Infrared spectroscopy allows for the comparison of the donor/acceptor properties of the amide groups fused to the acyl hydrazone versus the regular BTA amide groups. For **a-BTA** the NH I stretch is typically found at 3307 cm^{-1}, the C=O stretch at 1644 cm^{-1}, and amide II at 1532 cm^{-1}, indicative of lateral intermolecular hydrogen bonding in the bulk (Figure S3).[55] The mono acyl hydrazone derivative **m-BTA** bears two different types of amides, and also two corresponding NH I bands were observed at 3291 and 3187 cm^{-1}. The C=O band was found at 1649 cm^{-1} and amide II at 1545 cm^{-1}, slightly shifted compared to **a-BTA**. These results imply that the two types of amide groups possess different donor/acceptor properties, which will most likely also affect their ability and mechanism of polymerization into supramolecular aggregates.

Homoaggregation and Photoisomerization of m-BTA in Apolar Solvents. While **a-BTA** readily forms supramolecular polymers through 3-fold hydrogen bonding in apolar solvents such as methylcyclohexane (MCH), **m-BTA** monomers are molecularly dissolved at the same conditions. Even at concentrations higher than *c* = 1 mM in MCH no temperature-
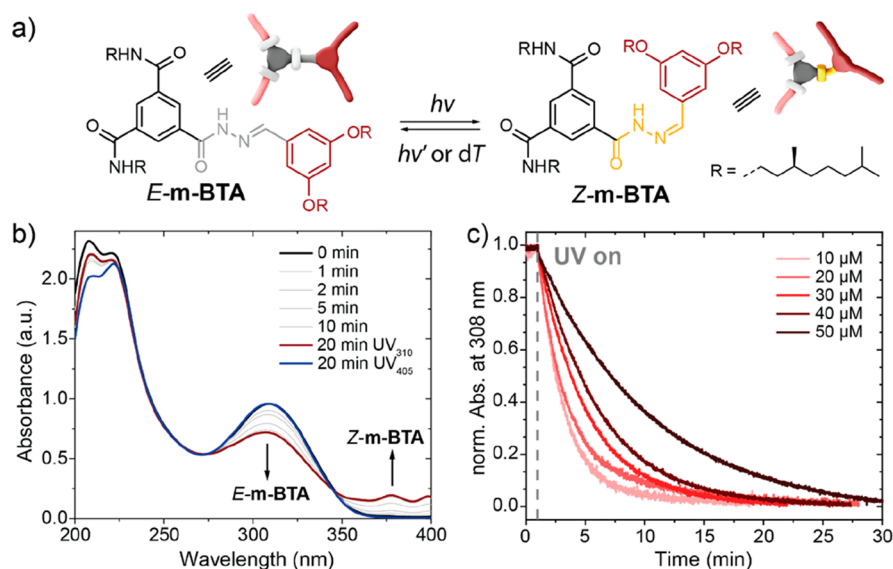
Figure 1. (a) Light-induced isomerization from the planar E isomer to the Z isomer of **m-BTA**. (b) Spectral changes with prolonged times of irradiation with UV light of λ = 310 or 405 nm. The band corresponding to the E isomer at λ = 308 nm decreases, and a new band from the Z isomer arises around λ = 375−405 nm when irradiated with UV_{310} (c = 50 μM in MCH). (c) Decrease of the E isomer band upon irradiation for solutions of c = 10−50 μM in MCH.
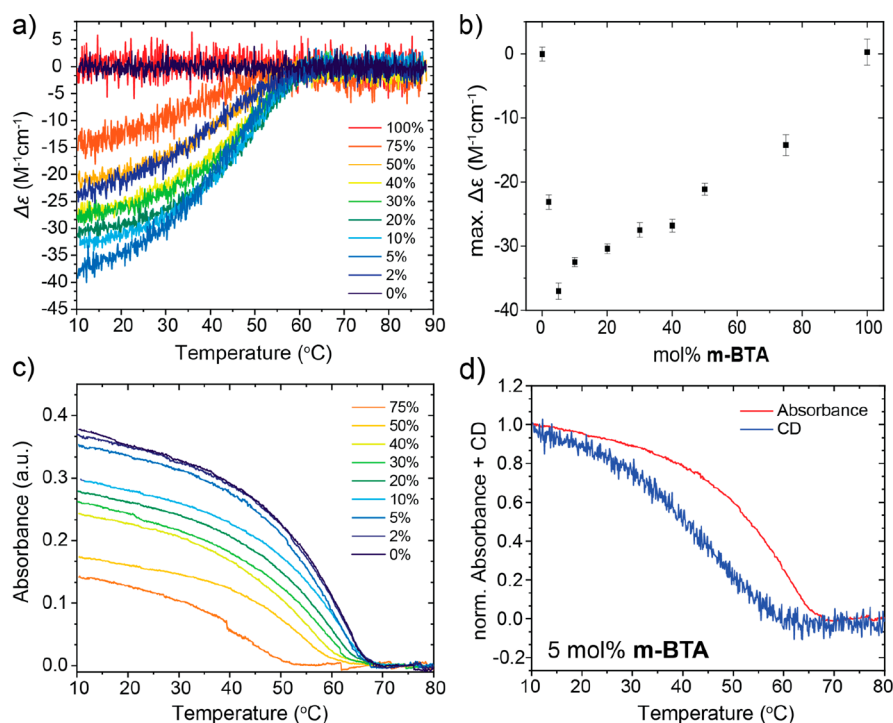

Figure 2. Copolymerization of chiral acyl hydrazone functionalized E-**m-BTA** with **a-BTA**. (a) CD melting curves of copolymer mixtures (cooling rate = 1 K min^{-1}). (b) CD maximum determined by averaging the $\Delta\varepsilon$ value at 223 nm in (a) between 10 and 15 °C for the different ratios of E-**m-BTA**/**a-BTA** (error bars indicate standard deviation). (c) UV melting curves showing decrease in T_e with increasing mol % E-**m-BTA** of the copolymer mixtures. (d) Normalized CD and absorbance melting curves (c_{tot} = 25 μM in MCH, signal probed at λ = 223 nm).

dependent changes in the absorbance or circular dichroism (CD) signal were observed that would indicate aggregation. FT-IR experiments of **m-BTA** and **a-BTA** at 2.0 mM in MCH also found significantly different hydrogen-bonding patterns (Figure S4). While **a-BTA** exhibited a band at around 3250 and 1650 cm^{-1} typical for triple hydrogen bonded, helical arrangement in solution, for **m-BTA** those bands were not present or shifted, indicating that they are not assembled as **a-**

BTA. To investigate the E to Z isomerization of the acyl hydrazone monomer (Figure 1a), solutions of **m-BTA** in MCH were irradiated with UV light (λ = 310 nm) for 1 min periods during the first 5 min and then for longer periods until 20 min of total irradiation time. Absorbance spectra were recorded after each irradiation step. In the absorbance spectra, the band of E-**m-BTA** at λ = 308 nm decreased, and a new
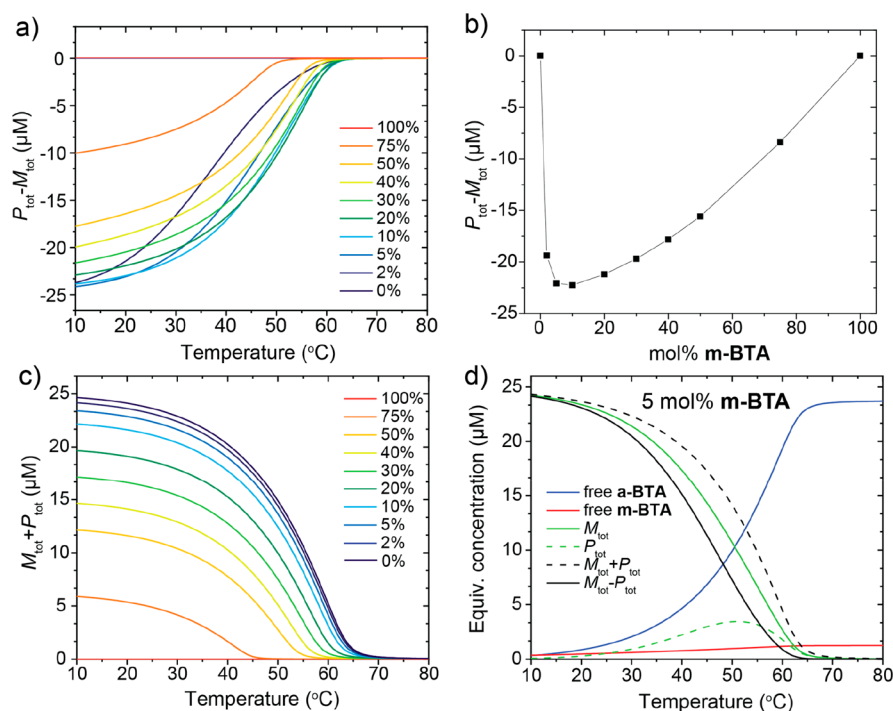
Figure 3. Theoretical modeling of the copolymerization of E-**m**-BTA/**a**-BTA. (a) Calculated $P_{tot} - M_{tot}$ over a range of temperatures (curves of 0 and 100 mol % **m**-BTA overlap at zero) and (b) with increasing mol % **m**-BTA at 25 °C. (c) $M_{tot} + P_{tot}$ curves for the copolymer mixtures with increasing mol % of E-**m**-BTA. (d) Specimen plot of a 5 mol % mixture of E-**m**-BTA in **a**-BTA (calculations based on $c_{tot} = 25$ μM in MCH, $\Delta H_{MAB} = -46.5$ kJ mol^{-1}, $\Delta S_{AB} = -54.2$ J mol^{-1} K^{-1}, and $\Delta H_{P}^{pen} = 2$ kJ mol^{-1}).

broad band at $\lambda = 375-405$ nm corresponding to the Z-**m**-BTA appeared (Figure 1b).

To investigate the kinetics of the isomerization, the wavelength of maximum absorption of E-**m**-BTA at $\lambda = 308$ nm was monitored over time while irradiating with UV light in situ (Figure 1c). Initially, the band decreases rapidly until a plateau is reached at around half an hour at a concentration of $c = 50$ μM **m**-BTA. Irradiation with UV light of $\lambda = 405$ nm reverses the process, and the original absorbance spectrum is recovered.[46] To prepare an effective, photoresponsive material, the reversibility of the photoswitch is crucial. Therefore, the switching cycle was repeated up to six times without visible fatigue of the acyl hydrazone monomers (Figure S5). The thermal half-time of the photoswitch was determined to be $t_{1/2} = 2.3$ h by monitoring the recovery of the E-**m**-BTA band over time at 25 °C (Figure S6). The switching of **m**-BTA can thus be reversed by light or by thermal equilibration.

Spectroscopic Investigation of the Copolymerization of m-BTA and a-BTA. The molecular structure of **m**-BTA is similar to alkyl BTAs such as **a**-BTA, with two aliphatic side chains connected on the amide groups of the central core. Upon mixing 5 mol % of E-**m**-BTA with **a**-BTA, we discovered that a copolymer was formed through cooperative supramolecular copolymerization with a strong CD signal at $\lambda_{max} = 223$ nm (Figure S9 and Figure 2a). The E-**m**-BTA monomers serve as chiral sergeants and dictate the formation of helical aggregates with a helical bias in the coassembly with **a**-BTAs. To understand the mixing of the two components, we prepared a number of copolymer solutions with increasing mol % E-**m**-BTA, keeping the total monomer concentration constant at $c_{tot} = 25$ μM. The amplification of chirality in these Sergeants-and-Soldiers experiments reaches its maximum CD effect of $\Delta\varepsilon = -38$ M^{-1} cm^{-1} at around 5 mol % E-**m**-BTA in the assembly,

which is comparable to the amplification of chirality with chiral alkyl BTAs or related BTA based monomers previously reported by our group.[56,59] Interestingly, the maximum CD value measured for the copolymer mixtures ($c_{tot} = 25$ μM in MCH) initially increases with increasing percentages of chiral comonomer (2−5 mol % **m**-BTA) but decreases with higher percentages of comonomer (10−100 mol %, Figure 2b). As the **m**-BTA monomers do not homopolymerize but form copolymers, we concluded that they act as an intercalator in the **a**-BTA stacks. An intercalator, unlike a comonomer, can insert between monomers of a different type but has no affinity to form homoaggregates. At high mol % of E-**m**-BTA, the CD signal therefore decreases as there is less **a**-BTA monomer available for aggregate formation. The shape of the CD spectra observed for the copolymer mixtures resembles the shape obtained with low quantities of chiral alkyl BTAs with no additional Cotton effect at the $\pi-\pi^*$ transition absorbance band at $\lambda = 308$ nm of the hydrazone chromophore (Figure S9).[52] Remarkably, the chiral side chains of **m**-BTA dictate the helicity of the copolymer stacks, while the $\pi-\pi^*$ transition of the acyl hydrazone is optically inactive.

The temperature of elongation (T_e) at which the elongation of supramolecular polymers becomes favorable can be determined from variable-temperature UV experiments. For copolymer mixtures the experimentally found T_e decreases with addition of the intercalator E-**m**-BTA (Figure 2c and Figure S8) but less than with pure dilution of **a**-BTA (Figures S7 and S8). This result indicates that the two monomers copolymerize. When comparing the T_e obtained from variable-temperature CD and UV experiments, for 5 mol % E-**m**-BTA mixed with **a**-BTA a difference of around 8 °C can be observed, suggesting that at 65 °C both P- and M-helices are formed, and only at lower temperature the helicity is fully

biased by the sergeants (Figure 2d). This difference in T_e becomes less pronounced with increasing ratio of *E*-**m-BTA** (Figure S10).

Theoretical Modeling of Copolymerization. To understand the underlying mechanism and effects of the comonomer on the chain length, we employed the copolymerization mass-balance model previously published.[61,62] With this general model, we describe the two-component assembly of **m-BTA** and **a-BTA**. As a first step, a dilution series of the homopolymerization of **a-BTA** (monomer *A* in the model) is investigated, assuming that the monomers assemble in equal number of *M*- and *P*-aggregates. From the experimental melting curves of **a-BTA**, the thermodynamic parameters obtained for enthalpy (ΔH_{AA}), entropy (ΔS_{AA}), and nucleation penalty (ΔH_{nuc}^{pen}) were identical to the values previously reported by Das et al.[60] Using those values, the model predicts the degree of polymerization (Φ) of the homopolymers of pure soldier **a-BTA** and the polymer length at different concentrations and temperatures (Figures S11 and S12).

Next, the case of a two-component assembly with *E*-**m-BTA** (monomer *B* in the model) intercalating into the stacks of **a-BTA** was considered. The *E*-**m-BTA** monomers are chiral, so preferential mixing into *M*-type aggregates is assumed by setting a penalty for mixing into *P*-helices. As **m-BTA** does not homopolymerize, only *A*−*B* or *B*−*A* bonds can be formed, but no *B*−*B* bonds, i.e., the property of an intercalator. We express the Gibbs free energy changes of these hetero bond formations in an enthalpy (ΔH_{MAB}) and an entropy (ΔS_{MAB}) parameter as well as an additional mismatch penalty (ΔH_P^{pen}) for mixing into the nonpreferred helical aggregate type for the copolymer system (see the Supporting Information for details). Consecutively, the temperature-dependent melting curves and distributions of species for the different copolymer mixtures can be calculated (Figure 3a−d and Figures S14−S16). The calculated curves are in good agreement with the experimental curves. Similar to the experimentally observed difference in T_e from UV or CD curves, the model also shows the difference in helical bias when comparing the total number of monomers in aggregates ($M_{tot} + P_{tot}$) with the difference in the number of monomers in aggregates of unpreferred and preferred helicity ($M_{tot} - P_{tot}$, Figure 3d and Figure S16). The model also predicts an initial increase in polymer length at low sergeant concentrations (2−10 mol % *E*-**m-BTA**) due to the preferred formation of *M*-aggregates followed by a decrease in length from higher sergeant concentrations (20−75 mol %) when more intercalator than monomer is present (Figure S15).

Light-Induced Chain Length Modulation of a-BTA Polymers with m-BTA. After establishing the intercalation of *E*-**m-BTA** into **a-BTA** stacks, we studied the consequences of the photoisomerization of *E*-**m-BTA** into *Z*-**m-BTA** in the coassembly with **a-BTA** (inert comonomer) on the length and structure of the copolymers. Because of the sensitivity of the supramolecular systems to external triggers, it is hypothesized that the isomerization of small amounts of photoresponsive monomers in the copolymer should be sufficient to affect the overall assembly, through amplification of the stimulus in the cooperative **a-BTA** system.

Upon irradiation of a copolymer gel (6 wt % in MCH, c_{tot} = 66 mM) of **a-BTA** doped with 10 mol % **m-BTA**, a macroscopic phase transformation from the gel to a liquid was induced, although 99.4% of the organogel is inert to light (Figure 4). The process is fully reversible by heating to 90 °C or irradiation with UV$_{405}$ light and allowing for re-equilibration
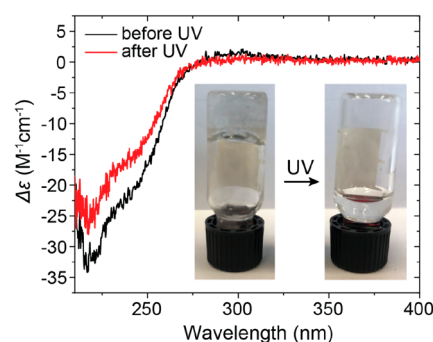

Figure 4. Effect of light irradiation on **m-BTA/a-BTA** copolymers. (a) Decrease in CD intensity of 10 mol % **m-BTA** in **a-BTA** after 15 min of UV$_{310}$ irradiation (c_{tot} = 25 μM in MCH). Inset: gel-to-sol transformation of a copolymer gel of 10 mol % **m-BTA** in **a-BTA** (6 wt % in MCH) upon irradiation.

at room temperature for 2 h. After the isomerization cycle a stable gel was recovered, which could withstand the tube inversion test. In a control experiment with a homopolymer gel of the same effective **a-BTA** concentration (5.4 wt % in MCH), no changes were observed before and after irradiation. The photoisomerization of a small amount (0.6 wt %) of photoresponsive monomers of the coassembly appears to be enough to locally break the network of fibers and reach the threshold of the sol−gel transition, expressed visibly on the macroscopic scale by the destruction of the gel.[27] Similar experiments performed at c_{tot} = 25 μM showed minor changes in the CD spectrum before and after irradiation (Figure 4). The equilibration and chiral amplification when adding either *E*- or *Z*-**m-BTA** to a solution of **a-BTA** occurred within seconds, suggesting a highly dynamic exchange and interactions of both isomers with the **a-BTA** stacks. This result together with the gel-to-sol transition suggests that the *Z*-**m-BTA** isomers still coassemble with **a-BTA** but decrease the fiber length. We hypothesize that **m-BTA** transforms from an intercalator to a chain capper of the **a-BTA** stacks upon isomerization from *E*-**m-BTA** into the *Z*-**m-BTA** isomer, where the nonplanar *Z*-**m-BTA** monomer blocks the chain ends to further addition of a monomer through steric hindrance. As a result, the average degree of polymerization (Φ, average amount of monomers per polymer) will decrease as evidenced by the sol−gel transformation. The average degree of aggregation (α, fraction of monomers in an aggregate), however, should be less affected, as most monomers are still in an aggregate, though shorter in length.

Static Light Scattering Reveals Changes in Chain Length. To probe the effects of irradiation on the average degree of polymerization and to confirm the role of *Z*-**m-BTA** as a chain capper, we conducted a series of static light scattering (SLS) experiments. To determine the length of the copolymers, scattering curves of **m-BTA/aBTA** copolymers (2−50 mol % **m-BTA**, c_{tot} = 2.0 mM in MCH) were measured (Figure 5a). The experimental curves were fitted with a cylindrical model to obtain the length of the aggregates.[63] Scattering profiles were recorded before, after UV$_{310}$ (*E* to *Z* isomerization) and after UV$_{405}$ irradiation (*Z* to *E* back-isomerization) for all copolymer ratios (Figure S22) to show the difference in length for the intercalator and chain capper cases. Additionally, we measured the Rayleigh ratio (R_θ) at a fixed angle to monitor the progress of photoisomerization in real time (Figure 5b, Figures S20 and S21). For 10 mol % of
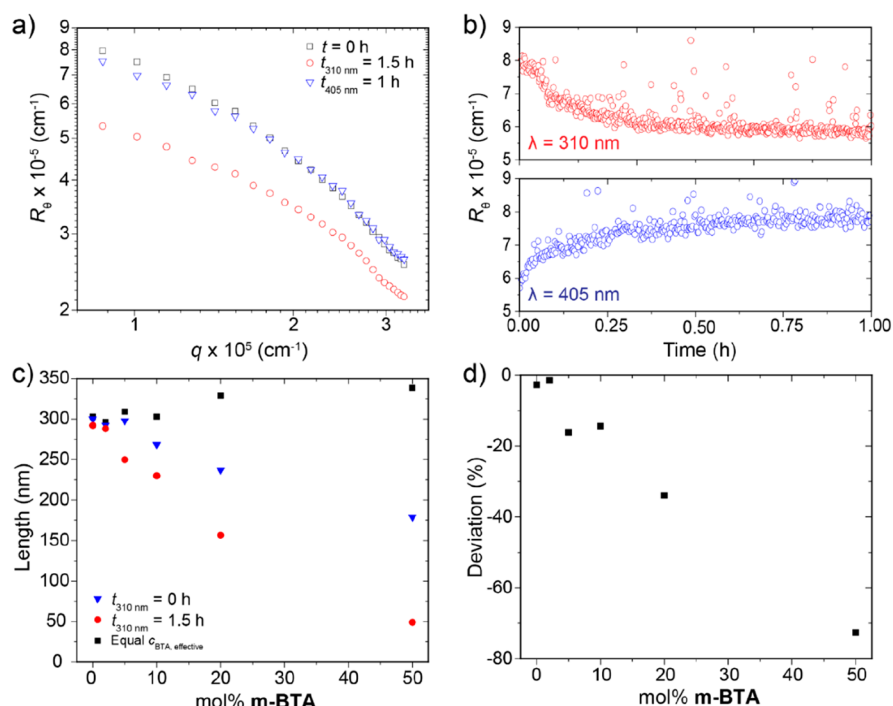
Figure 5. Decrease in copolymer length determined by SLS when switching **m-BTA** from an intercalating comonomer (*E*-**m-BTA**) to a chain capper (*Z*-**m-BTA**) with light. (a) Scattering profiles of 10 mol % **m-BTA** in **a-BTA** before, after UV$_{310}$, and after UV$_{405}$ irradiation. (b) Decrease in R_θ for 5 mol % **m-BTA** in **a-BTA** at an angle of 30° followed during *E* to *Z* isomerization and *Z* to *E* back-isomerization. (c) Effect of light stimulus on the chain length of the copolymers of **m-BTA/a-BTA** over a range of copolymer compositions. (d) Deviation of chain length in **a-BTA/m-BTA** stacks before and after irradiation with increasing mol % **m-BTA**. Total concentration was c = 2.0 mM in MCH in all cases.

m-BTA in **a-BTA**, the weight-average length decreases from approximately 269 to 230 nm by UV$_{310}$ irradiation. When isomerizing back from *Z* to *E* isomers with UV$_{405}$ irradiation, R_θ increases until the scattering profile overlaps with the nonirradiated sample (Figure 5a,c), which suggests that the length and morphology of the aggregates is the same as for the nonirradiated samples and that the process is reversible.

To quantify the changes in chain length upon mixing and photoisomerization, the copolymer mixtures were compared to pure diluted **a-BTA** samples of the same effective concentration (c_{eff}), not containing the photoresponsive **m-BTA** comonomer. The polymer length for the samples of same c_{eff} remains constant, only a slight increase is observed as we measure slightly above the critical entanglement concentration of the fibers to keep a good signal-to-noise ratio (Figure 5c, black squares).[63] In accordance with the predictions from the theoretical model, we observe that copolymers of *E*-**m-BTA**/**a-BTA** show a decrease in length above 10 mol % of *E*-**m-BTA** intercalating to the stacks (Figure 5c, blue triangles) due to the decrease of **a-BTA** concentration and the destabilization of the **a-BTA/m-BTA** stacks.

When irradiating the solutions, a decrease in length is observed for all **m-BTA/a-BTA** mixtures (Figure 5c, red dots). The decrease in length becomes more pronounced with increasing mol % of **m-BTA**. The plot of the percentage of deviation in chain lengths before and after irradiation clearly shows the large changes in polymer length, which we attribute to the transformation of **m-BTA** comonomers from intercalators to chain cappers (Figure 5d).

These observations were rationalized by using the thermodynamic model. To describe the two-component system after photoisomerization, the model was extended for *Z*-**m-BTA** acting as a chain capper by prohibiting the formation of *B*−*A* bonds as additional assumption. Aggregates with *B* monomers at the chain end thus cannot grow further. For this chain-capping case, the model predicts a decrease in mean aggregate length with increasing mol % of chain capper, which is even stronger than the experimentally observed effect (Figure S18). The model used for understanding the coassembly of *E*-**m-BTA** in the **a-BTA** stacks assumes that the system is always at thermodynamic equilibrium and that 100% of *E*-**m-BTA** converts to *Z*-**m-BTA**. Because of the thermal reisomerization of the chain capper *Z*-**m-BTA** over time, this assumption does not hold, which makes an exact prediction of the degree of polymerization difficult.

■ DISCUSSION

With the insights obtained from the spectroscopy and SLS data combined with the theoretical model, we can control the influence of the second component **m-BTA** on the chain length of the supramolecular copolymer with *E*-**m-BTA** acting as an intercalator and *Z*-**m-BTA** as a chain capper. Moreover, it is demonstrated that polymer length is highly dependent on the concentration regime and that the composition of the system changes with concentration. The polymer chain length was calculated with the model over a range of concentrations from 25 μM to 40 mM with increasing mol % of additive **m-BTA** (Figure S18). The predicted length was then normalized to the value for the polymer length at 0 mol % **m-BTA** for all concentrations to visualize the relative changes over the concentrations (Figure 6). For the simplest case of dilution of pure **a-BTA**, the length decreases and scales with the square root of the concentration. Therefore, the decrease in normalized length is identical for the five concentrations plotted in Figure 6 (black lines) although the non-normalized lengths differ (Figure S18). When *E*-**m-BTA** acts as an
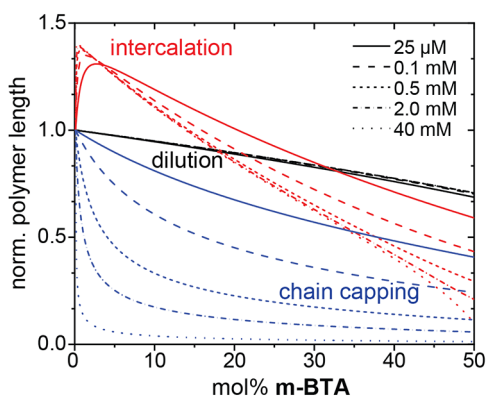
Figure 6. Influence of concentration on decrease of chain length for dilution of **a-BTA** (black lines), for **m-BTA** as an intercalator (red lines), and as a chain capper (blue lines). The effects of the additive on the chain length predicted by the thermodynamic model are small at lower concentrations but become much more pronounced at higher concentration.

intercalator (red lines), the chain length varies in two regimes. At first, the chain length increases when predominantly *M*-type helices are formed at the expense of *P*-type helices by intercalation of the chiral comonomer. From roughly 20 mol % of *E*-**m-BTA** intercalator, the copolymers are shorter than the pure **a-BTA** aggregates of the dilution series at the same effective concentration because of the decrease of **a-BTA** concentration and the destabilization of the **m-BTA/a-BTA** copolymers. At low overall concentrations, the decrease in chain length is not very pronounced. At higher concentrations, however, the length decreases more dramatically, and up to 75% length decrease is observed at 40 mM by mere intercalation of *E*-**m-BTA**. When *Z*-**m-BTA** acts as a chain capper (blue lines), this trend becomes even more apparent. While at 25 μM with 50 mol % chain capper added the normalized length decreases to roughly 45% of the original length, at 40 mM the chains shorten to around 6% of the original length for as low as 5 mol % of chain capper.

Contrary to chain capping in covalent polymers where the ratio of chain capper to monomer controls the chain length, in supramolecular polymers also the concentration, and not just the ratio of chain capper to monomer, majorly affects the aggregate length.[8] This strong dependence on concentration might seem counterintuitive at first, as it makes the characterization of two-component systems more complex. The analytical techniques used to characterize chain length in supramolecular systems require different concentration regimes, ranging from 25 μM for CD spectroscopy, over 2.0 mM for SLS, to 6 wt % (~60 mM) for the organogel. This demonstrates that one has to be careful when interpreting data from analytical techniques over a range of concentrations as the results are significantly affected by the concentration regime.

CONCLUSION

In conclusion, we reported on the copolymerization at thermodynamic equilibrium of achiral alkyl BTAs with a chiral, photoresponsive acyl hydrazone BTA monomer that plays a dual role in the assembly. While *E*-**m-BTA** does not form homopolymers, it intercalates into the **a-BTA** aggregates, inducing a preferred helical sense in the stacks. Upon photoirradiation from the *E* to the *Z* isomer, **m-BTA** reversibly

transforms from an intercalator to a chain capper, effectively reducing the average chain length and leading to a macroscopic sol-to-gel transition. By theoretical modeling of the system, we could gain insights into the state of the assembly before and after light stimulus. The model was also used to demonstrate the effect of an intercalator and a chain capper in a two-component copolymerization over a broad range of concentrations. The theoretical predictions show that the influence of an additive becomes more and more dramatic with increasing average chain length at higher concentrations.

The present work provides a strategy to control the length and the composition of cooperative supramolecular polymers by using a small amount of responsive comonomer. In the quest for functional out-of-equilibrium systems, new insights are given to translate small molecular changes into macroscopic phase transitions. Moreover, these results highlight the sensitivity of supramolecular systems to concentration and the necessity to characterize supramolecular polymers using various techniques in different concentration regimes.

■ ASSOCIATED CONTENT

Ⓢ Supporting Information

The Supporting Information is available free of charge at https://pubs.acs.org/doi/10.1021/jacs.0c00858.

Experimental procedures, characterization data, details on theoretical modeling, and Figures S1−S27 (PDF)

■ AUTHOR INFORMATION

Corresponding Author

  E. W. Meijer − *Laboratory of Macromolecular and Organic Chemistry and Institute for Complex Molecular Systems (ICMS), Eindhoven University of Technology, 5600 MB Eindhoven, The Netherlands;* ⓞ orcid.org/0000-0003-4126-7492; Email: e.w.meijer@tue.nl

Authors

  Elisabeth Weyandt − *Laboratory of Macromolecular and Organic Chemistry and Institute for Complex Molecular Systems (ICMS), Eindhoven University of Technology, 5600 MB Eindhoven, The Netherlands*

  Gijs M. ter Huurne − *Laboratory of Macromolecular and Organic Chemistry and Institute for Complex Molecular Systems (ICMS), Eindhoven University of Technology, 5600 MB Eindhoven, The Netherlands*

  Ghislaine Vantomme − *Laboratory of Macromolecular and Organic Chemistry and Institute for Complex Molecular Systems (ICMS), Eindhoven University of Technology, 5600 MB Eindhoven, The Netherlands;* ⓞ orcid.org/0000-0003-2036-8892

  Albert J. Markvoort − *Institute for Complex Molecular Systems (ICMS) and Computational Biology Group, Eindhoven University of Technology, 5600 MB Eindhoven, The Netherlands;* ⓞ orcid.org/0000-0001-6025-9557

  Anja R. A. Palmans − *Laboratory of Macromolecular and Organic Chemistry and Institute for Complex Molecular Systems (ICMS), Eindhoven University of Technology, 5600 MB Eindhoven, The Netherlands;* ⓞ orcid.org/0000-0002-7201-1548

Complete contact information is available at:
https://pubs.acs.org/10.1021/jacs.0c00858

Notes

The authors declare no competing financial interest.

■ REFERENCES

(1) Adelizzi, B.; Van Zee, N. J.; de Windt, L. N. J.; Palmans, A. R. A.; Meijer, E. W. Future of Supramolecular Copolymers Unveiled by Reflecting on Covalent Copolymerization. *J. Am. Chem. Soc.* **2019**, *141* (15), 6110−6121.

(2) Yang, L.; Tan, X.; Wang, Z.; Zhang, X. Supramolecular Polymers: Historical Development, Preparation, Characterization, and Functions. *Chem. Rev.* **2015**, *115* (15), 7196−7239.

(3) Vantomme, G.; Meijer, E. W. The Construction of Supramolecular Systems. *Science (Washington, DC, U. S.)* **2019**, *363* (6434), 1396−1397.

(4) Michelsen, U.; Hunter, C. A. Self-Assembled Porphyrin Polymers. *Angew. Chem., Int. Ed.* **2000**, *39* (4), 764−767.

(5) Sijbesma, R. P.; Beijer, F. H.; Brunsveld, L.; Folmer, B. J.; Hirschberg, J. H.; Lange, R. F.; Lowe, J. K.; Meijer, E. W. Reversible Polymers Formed from Self-Complementary Monomers Using Quadruple Hydrogen Bonding. *Science* **1997**, *278* (5343), 1601−1604.

(6) Bellot, M.; Bouteiller, L. Thermodynamic Description of Bis-Urea Self-Assembly: Competition between Two Supramolecular Polymers. *Langmuir* **2008**, *24* (24), 14176−14182.

(7) Lortie, F.; Boileau, S.; Bouteiller, L.; Chassenieux, C.; Lauprêtre, F. Chain Stopper-Assisted Characterization of Supramolecular Polymers. *Macromolecules* **2005**, *38* (12), 5283−5287.

(8) Knoben, W.; Besseling, N. A. M.; Bouteiller, L.; Cohen Stuart, M. A. Dynamics of Reversible Supramolecular Polymers: Independent Determination of the Dependence of Linear Viscoelasticity on Concentration and Chain Length by Using Chain Stoppers. *Phys. Chem. Chem. Phys.* **2005**, *7* (11), 2390.

(9) De Greef, T. F. A.; Smulders, M. M. J.; Wolffs, M.; Schenning, A. P. H. J.; Sijbesma, R. P.; Meijer, E. W. Supramolecular Polymerization. *Chem. Rev.* **2009**, *109* (11), 5687−5754.

(10) Ogi, S.; Sugiyasu, K.; Manna, S.; Samitsu, S.; Takeuchi, M. Living Supramolecular Polymerization Realized through a Biomimetic Approach. *Nat. Chem.* **2014**, *6* (3), 188−195.

(11) Ogi, S.; Stepanenko, V.; Sugiyasu, K.; Takeuchi, M.; Würthner, F. Mechanism of Self-Assembly Process and Seeded Supramolecular Polymerization of Perylene Bisimide Organogelator. *J. Am. Chem. Soc.* **2015**, *137* (9), 3300−3307.

(12) Kang, J.; Miyajima, D.; Mori, T.; Inoue, Y.; Itoh, Y.; Aida, T. A Rational Strategy for the Realization of Chain-Growth Supramolecular Polymerization. *Science (Washington, DC, U. S.)* **2015**, *347* (6222), 646−651.

(13) Endo, M.; Fukui, T.; Jung, S. H.; Yagai, S.; Takeuchi, M.; Sugiyasu, K. Photoregulated Living Supramolecular Polymerization Established by Combining Energy Landscapes of Photoisomerization and Nucleation−Elongation Processes. *J. Am. Chem. Soc.* **2016**, *138* (43), 14347−14353.

(14) Matsubara, S.; Tamiaki, H. Phototriggered Dynamic and Biomimetic Growth of Chlorosomal Self-Aggregates. *J. Am. Chem. Soc.* **2019**, *141* (3), 1207−1211.

(15) Vantomme, G.; ter Huurne, G. M.; Kulkarni, C.; ten Eikelder, H. M. M.; Markvoort, A. J.; Palmans, A. R. A.; Meijer, E. W. Tuning the Length of Cooperative Supramolecular Polymers under Thermodynamic Control. *J. Am. Chem. Soc.* **2019**, *141* (45), 18278−18285.

(16) Fredy, J. W.; Méndez-Ardoy, A.; Kwangmettatam, S.; Bochicchio, D.; Matt, B.; Stuart, M. C. A.; Huskens, J.; Katsonis, N.; Pavan, G. M.; Kudernac, T. Molecular Photoswitches Mediating the Strain-Driven Disassembly of Supramolecular Tubules. *Proc. Natl. Acad. Sci. U. S. A.* **2017**, *114* (45), 11850−11855.

(17) Bochicchio, D.; Kwangmettatam, S.; Kudernac, T.; Pavan, G. M. How Defects Control the Out-of-Equilibrium Dissipative Evolution of a Supramolecular Tubule. *ACS Nano* **2019**, *13* (4), 4322−4334.

(18) Nelson, A. Engineering Interactions. *Nat. Mater.* **2008**, *7* (7), 523−525.

(19) Yan, X.; Wang, F.; Zheng, B.; Huang, F. Stimuli-Responsive Supramolecular Polymeric Materials. *Chem. Soc. Rev.* **2012**, *41* (18), 6042.

(20) White, T. J.; Broer, D. J. Programmable and Adaptive Mechanics with Liquid Crystal Polymer Networks and Elastomers. *Nat. Mater.* **2015**, *14* (11), 1087−1098.

(21) Kocak, G.; Tuncer, C.; Bütün, V. pH-Responsive Polymers. *Polym. Chem.* **2017**, *8* (1), 144−176.

(22) Ridi, F.; Bonini, M.; Baglioni, P. Magneto-Responsive Nanocomposites: Preparation and Integration of Magnetic Nanoparticles into Films, Capsules, and Gels. *Adv. Colloid Interface Sci.* **2014**, *207* (1), 3−13.

(23) Yao, X.; Li, T.; Wang, J.; Ma, X.; Tian, H. Recent Progress in Photoswitchable Supramolecular Self-Assembling Systems. *Adv. Opt. Mater.* **2016**, *4* (9), 1322−1349.

(24) Yagai, S.; Kitamura, A. Recent Advances in Photoresponsive Supramolecular Self-Assemblies. *Chem. Soc. Rev.* **2008**, *37* (8), 1520.

(25) Zhang, Q.; Qu, D.-H.; Tian, H. Photo-Regulated Supramolecular Polymers: Shining Beyond Disassembly and Reassembly. *Adv. Opt. Mater.* **2019**, *7* (16), 1900033.

(26) Eelkema, R. Photo-Responsive Doped Cholesteric Liquid Crystals. *Liq. Cryst.* **2011**, *38* (11−12), 1641−1652.

(27) Draper, E. R.; Adams, D. J. Photoresponsive Gelators. *Chem. Commun.* **2016**, *52* (53), 8196−8206.

(28) Russew, M.-M.; Hecht, S. Photoswitches: From Molecules to Materials. *Adv. Mater.* **2010**, *22* (31), 3348−3360.

(29) Moran, M. J.; Magrini, M.; Walba, D. M.; Aprahamian, I. Driving a Liquid Crystal Phase Transition Using a Photochromic Hydrazone. *J. Am. Chem. Soc.* **2018**, *140* (42), 13623−13627.

(30) Ryabchun, A.; Li, Q.; Lancia, F.; Aprahamian, I.; Katsonis, N. Shape-Persistent Actuators from Hydrazone Photoswitches. *J. Am. Chem. Soc.* **2019**, *141* (3), 1196−1200.

(31) Pijper, D.; Jongejan, M. G. M.; Meetsma, A.; Feringa, B. L. Light-Controlled Supramolecular Helicity of a Liquid Crystalline Phase Using a Helical Polymer Functionalized with a Single Chiroptical Molecular Switch. *J. Am. Chem. Soc.* **2008**, *130* (13), 4541−4552.

(32) Sackmann, E. Photochemically Induced Reversible Color Changes in Cholesteric Liquid Crystals. *J. Am. Chem. Soc.* **1971**, *93* (25), 7088−7090.

(33) Achalkumar, A. S.; Hiremath, U. S.; Rao, D. S. S.; Prasad, S. K.; Yelamaggad, C. V. Self-Assembly of Hekates-Tris(N-Salicylideneaniline)s into Columnar Structures: Synthesis and Characterization. *J. Org. Chem.* **2013**, *78* (2), 527−544.

(34) Li, T.; Li, X.; Wang, J.; Ågren, H.; Ma, X.; Tian, H. Photoresponsive Supramolecular Assemblies Based on a C3-Symmetric Benzene-1,3,5-Tricarboxamide-Anchored Diarylethene. *Adv. Opt. Mater.* **2016**, *4* (6), 840−847.

(35) Heerdt, G.; Tranca, I.; Markvoort, A. J.; Szyja, B. M.; Morgon, N. H.; Hensen, E. J. M. Photoisomerization Induced Scission of Rod-

like Micelles Unravelled with Multiscale Modeling. *J. Colloid Interface Sci.* **2018**, *510*, 357−367.

(36) Zhou, Y.; Xu, M.; Yi, T.; Xiao, S.; Zhou, Z.; Li, F.; Huang, C. Morphology-Tunable and Photoresponsive Properties in a Self-Assembled Two-Component Gel System. *Langmuir* **2007**, *23* (1), 202−208.

(37) Ji, L.; Ouyang, G.; Liu, M. Binary Supramolecular Gel of Achiral Azobenzene with a Chaperone Gelator: Chirality Transfer, Tuned Morphology, and Chiroptical Property. *Langmuir* **2017**, *33*, 12419−12426.

(38) Pieraccini, S.; Campitiello, M.; Carducci, F.; Davis, J. T.; Mariani, P.; Masiero, S. Playing Supramolecular Dominoes with Light: Building and Breaking a Photoreversible G-Quadruplex Made from Guanosine, Boric Acid and an Azobenzene. *Org. Biomol. Chem.* **2019**, *17* (10), 2759−2769.

(39) Georgiev, V. N.; Grafmüller, A.; Bléger, D.; Hecht, S.; Kunstmann, S.; Barbirz, S.; Lipowsky, R.; Dimova, R. Area Increase and Budding in Giant Vesicles Triggered by Light: Behind the Scene. *Adv. Sci.* **2018**, *5* (8), 1800432.

(40) Karunakaran, S. C.; Cafferty, B. J.; Jain, K. S.; Schuster, G. B.; Hud, N. V. Reversible Transformation of a Supramolecular Hydrogel by Redox Switching of Methylene Blue—A Noncovalent Chain Stopper. *ACS Omega* **2020**, *5* (1), 344−349.

(41) Su, X.; Aprahamian, I. Hydrazone-Based Switches, Metallo-Assemblies and Sensors. *Chem. Soc. Rev.* **2014**, *43* (6), 1963.

(42) Lehn, J. M. From Supramolecular Chemistry towards Constitutional Dynamic Chemistry and Adaptive Chemistry. *Chem. Soc. Rev.* **2007**, *36* (2), 151−160.

(43) Corbett, P. T.; Leclaire, J.; Vial, L.; West, K. R.; Wietor, J.-L.; Sanders, J. K. M.; Otto, S. Dynamic Combinatorial Chemistry. *Chem. Rev.* **2006**, *106* (9), 3652−3711.

(44) Bhat, V. T.; Caniard, A. M.; Luksch, T.; Brenk, R.; Campopiano, D. J.; Greaney, M. F. Nucleophilic Catalysis of Acylhydrazone Equilibration for Protein-Directed Dynamic Covalent Chemistry. *Nat. Chem.* **2010**, *2* (6), 490−497.

(45) Nguyen; Ivan Huc, R. Optimizing the Reversibility of Hydrazone Formation for Dynamic Combinatorial Chemistry. *Chem. Commun.* **2003**, *0* (8), 942.

(46) van Dijken, D. J.; Kovaricek, P.; Ihrig, S. P.; Hecht, S. Acylhydrazones as Widely Tunable Photoswitches. *J. Am. Chem. Soc.* **2015**, *137* (47), 14982−14991.

(47) Cvrtila, I.; Fanlo-Virgós, H.; Schaeffer, G.; Monreal Santiago, G.; Otto, S. Redox Control over Acyl Hydrazone Photoswitches. *J. Am. Chem. Soc.* **2017**, *139* (36), 12459−12465.

(48) Su, X.; Aprahamian, I. Chem Soc Rev Themed Issue: Supramolecular and Dynamic Covalent Reactivity Hydrazone-Based Switches, Metallo-Assemblies and Sensors. *Chem. Soc. Rev.* **2014**, *43* (43), 1963−1981.

(49) Boekhoven, J.; Poolman, J. M.; Maity, C.; Li, F.; van der Mee, L.; Minkenberg, C. B.; Mendes, E.; van Esch, J. H.; Eelkema, R. Catalytic Control over Supramolecular Gel Formation. *Nat. Chem.* **2013**, *5* (5), 433−437.

(50) Kassem, S.; Lee, A. T. L.; Leigh, D. A.; Marcos, V.; Palmer, L. I.; Pisano, S. Stereodivergent Synthesis with a Programmable Molecular Machine. *Nature* **2017**, *549* (7672), 374−378.

(51) Vantomme, G.; Lehn, J. M. Reversible Adaptation to Photoinduced Shape Switching by Oligomer-Macrocycle Interconversion with Component Selection in a Three-State Constitutional Dynamic System. *Chem. - Eur. J.* **2014**, *20* (49), 16188−16193.

(52) Landge, S. M.; Tkatchouk, E.; Benítez, D.; Lanfranchi, D. A.; Elhabiri, M.; Goddard, W. A.; Aprahamian, I. Isomerization Mechanism in Hydrazone-Based Rotary Switches: Lateral Shift, Rotation, or Tautomerization? *J. Am. Chem. Soc.* **2011**, *133*, 9812−9823.

(53) Day, A. C.; Whiting, M. C. Acetone Hydrazone. *Org. Synth.* **1988**, *50*, 10−12.

(54) Lefebvre, V.; Cailly, T.; Fabis, F.; Rault, S. Two-Step Synthesis of Substituted 3-Aminoindazoles from 2-Bromobenzonitriles. *J. Org. Chem.* **2010**, *75* (8), 2730−2732.

(55) Stals, P. J. M.; Smulders, M. M. J.; Martín-Rapún, R.; Palmans, A. R. A.; Meijer, E. W. Asymmetrically Substituted Benzene-1,3,5-Tricarboxamides: Self-Assembly and Odd-Even Effects in the Solid State and in Dilute Solution. *Chem. - Eur. J.* **2009**, *15* (9), 2071−2080.

(56) Palmans, A. R. A.; Vekemans, J. A. J. M.; Havinga, E. E.; Meijer, E. W. Sergeants-and-Soldiers Principle in Chiral Columnar Stacks of Disc-Shaped Molecules With C3 Symmetry. *Angew. Chem., Int. Ed. Engl.* **1997**, *36* (23), 2648−2651.

(57) Green, M. M.; Reidy, M. P.; Johnson, R. J.; Darling, G.; O'Leary, D. J.; Willson, G. Macromolecular Stereochemistry: The Out-of-Proportion Influence of Optically Active Comonomers on the Conformational Characteristics of Polyisocyanates. The Sergeants and Soldiers Experiment. *J. Am. Chem. Soc.* **1989**, *111* (16), 6452−6454.

(58) He, C.; Lin, Z.; He, Z.; Duan, C.; Xu, C.; Wang, Z.; Yan, C. Metal-Tunable Nanocages as Artificial Chemosensors. *Angew. Chem., Int. Ed.* **2008**, *47* (5), 877−881.

(59) Smulders, M. M. J.; Filot, I. A. W.; Leenders, J. M. A.; van der Schoot, P.; Palmans, A. R. A.; Schenning, A. P. H. J.; Meijer, E. W. Tuning the Extent of Chiral Amplification by Temperature in a Dynamic Supramolecular Polymer. *J. Am. Chem. Soc.* **2010**, *132* (2), 611−619.

(60) Das, A.; Vantomme, G.; Markvoort, A. J.; ten Eikelder, H. M. M.; Garcia-Iglesias, M.; Palmans, A. R. A.; Meijer, E. W. Supramolecular Copolymers: Structure and Composition Revealed by Theoretical Modeling. *J. Am. Chem. Soc.* **2017**, *139* (20), 7036−7044.

(61) ten Eikelder, H. M. M.; Adelizzi, B.; Palmans, A. R. A.; Markvoort, A. J. Equilibrium Model for Supramolecular Copolymerizations. *J. Phys. Chem. B* **2019**, *123* (30), 6627−6642.

(62) ten Eikelder, H. M. M.; Markvoort, A. J. Mass-Balance Models for Scrutinizing Supramolecular (Co)Polymerizations in Thermodynamic Equilibrium. *Acc. Chem. Res.* **2019**, *52* (12), 3465−3474.

(63) Knoben, W.; Besseling, N. A. M. M.; Cohen Stuart, M. A. Chain Stoppers in Reversible Supramolecular Polymer Solutions Studied by Static and Dynamic Light Scattering and Osmometry. *Macromolecules* **2006**, *39* (7), 2643−2653.